MRS Advances © 2017 Materials Research Society
DOI: 10.1557/adv.2017.489

Synthetic Biology in Aqueous Compartments at the Micro- and Nanoscale

J. Boreyko,[1] P. Caveney,[2,3] S. L. Norred,[2,3] C. Chin,[2,3] S.T. Retterer,[2,3,4] M.L. Simpson,[2,3] C.P. Collier[2,3]

[1] Virginia Polytechnic Institute and State University, Blacksburg, VA, 24060
[2] Center for Nanophase Materials Sciences, Oak Ridge National Laboratory, Oak Ridge, TN 37831
[3] Bredesen Center, University of Tennessee, Knoxville, TN 37996
[4] Biosciences Division, Oak Ridge National Laboratory, Oak Ridge, TN 37831

ABSTRACT

Aqueous two-phase systems and related emulsion-based structures defined within micro- and nanoscale environments enable a bottom-up synthetic biological approach to mimicking the dynamic compartmentation of biomaterial that naturally occurs within cells. Model systems we have developed to aid in understanding these phenomena include on-demand generation and triggering of reversible phase transitions in ATPS confined in microscale droplets, morphological changes in networks of femtoliter-volume aqueous droplet interface bilayers (DIBs) formulated in microfluidic channels, and temperature-driven phase transitions in interfacial lipid bilayer systems supported on micro and nanostructured substrates. For each of these cases, the dynamics were intimately linked to changes in the chemical potential of water, which becomes increasingly susceptible to confinement and crowding. At these length scales, where interfacial and surface areas predominate over compartment volumes, both evaporation and osmotic forces become enhanced relative to ideal dilute solutions. Consequences of confinement and crowding in cell-sized microcompartments for increasingly complex scenarios will be discussed, from single-molecule mobility measurements with fluorescence correlation spectroscopy to spatio-temporal modulation of resource sharing in cell-free gene expression bursting.

INTRODUCTION

Macromolecular crowding and confinement have numerous thermodynamic and kinetic consequences for biochemical reaction dynamics and reactivity compared to dilute, homogenous environments.[1-4] Macromolecular crowding may help regulate weak DNA-protein binding interactions, for example, though both thermodynamic and kinetic mechanisms.[5] The most significant thermodynamic effects are related to excluded-volume interactions, the consequence of a reduction of configuration entropy available to reactants, which increases activity coefficients, and favors more compact conformational transition states. In addition to entropy, other nonspecific interactions such as electrostatic or hydrophobic effects modulate energetics. Dynamics are affected by changes in mobility for reacting molecules in restricted environments. Crowding will tend to decelerate diffusion-limited (fast) associations and accelerate slow (transition state activated complex) associations. Anomalous diffusion, characterized by a mean square displacement of a diffusing molecule that does not increase linearly with time, has been predicted in simulations of confined and crowded systems, yet much experimental evidence indicates that diffusion of small to medium size molecules in cellular aqueous compartments is still predominantly Brownian in nature, with mobility affected significantly only for larger

macromolecules.[6,7] In general, crowding and confinement have many different consequences acting simultaneously, making it difficult to predict outcomes.

Advances in micro/nanofabrication have resulted in the development of increasingly realistic synthetic models of complex biological systems. Micro/nanofabricated structures can be configured to reproduce the spatially segregated and restricted environments found in nature, resulting in enhanced local concentrations and reaction rates compared to bulk values.[8,9] Compartmentalization of complex multistep biological processes spatially and temporally segregates elementary reaction steps, facilitating the establishment of non-equilibrium steady states, control of reaction network connectivity and signaling cascades, and feed-forward and feedback loops.[10]

In this report, we describe experiments that elucidate how synthetic micro- and nanostructured volumes and interfaces reminiscent of those found in complex natural systems can lead to emergent functionality not observable in the bulk. At these scales, surface areas to volume ratios are large, and interface interactions become increasingly important, not only affecting the chemical activity of reactants in solution, but also that of the water solvent itself. Examples range in complexity from the relatively simple: crowding and confinement-induced modulation of the diffusional mobility of single molecules, to the more complex: adaptation of resource sharing strategies of cell-free protein expression systems in increasingly restricted environments.

RESULTS AND DISCUSSION

The phase behavior of a macroscopic heterogeneous system is determined using Gibb's phase rule relating the number of independent intensive variables, such as reagent mole fraction, temperature, and pressure, to the number of components and phases at thermodynamic equilibrium. The chemical activity of all components in the system is given by the Gibbs-Duhem relation: $\mathrm{d}G = V\,\mathrm{d}p - S\,\mathrm{d}T + \sum_{i=1}^{N} \mu_i \mathrm{d}N_i$, where μ_i, the chemical potential of the i^{th} component, is the change in free energy with respect to the change in the amount of that component, with all other components held constant. At cellular scales, solute interactions with micro- and nanostructured surfaces and interfaces become increasingly important for understanding the phase behavior of complex biological systems. Surface area to volume ratios are large, not only affecting the chemical activity of solutes, but also the water solvent itself, for example, through changes in water partial pressures which affect osmotic stresses acting on macromolecular conformations and reactions. [11] A dual role for the solute emerges, first, for direct ligand binding with other molecules in the system, and second, for indirect effects which act on all components of the solution. Crowding can amplify these effects, by further sterically excluding solute from water-filled cavities or pockets in crowded solution, at membranes or interfaces, and even at the surface of a macromolecule itself. In this picture, the chemical potential, or equivalently, the change in free energy of a solute at a membrane, interface, or macromolecule can occur once there is a change in the ratio of solute molecules to water at these surfaces relative to the ratio in dilute solution. [11]

We employ two strategies to control and study the effects of changing water chemical potential in confined and crowded conditions, both based on devices fabricated using micromolding of polydimethylsiloxane (PDMS). The first strategy involves on-demand creation of one or more femtoliter-volume water-in-oil droplets in a microfluidic channel. At these scales, evaporation is efficient, due to the high surface area to volume ratio of droplets 2 to 5 μm in

diameter, and to the permeability of PDMS to water vapor pervaporated from the droplets. [12] Changing the chemical potential difference of water by first saturating the PDMS chip with water lowers the droplet shrinkage rate by over a factor of 40. To a limited extent, the choice of oil used can also have an effect, since the equilibrium aqueous droplet size depends on the partition function of water in the oil. The largest contributor to the spontaneous and dynamical behavior of individual microscale droplets, and between two or more droplets, is the interfacial tension and other capillary forces between the droplets and oil, and at the interfaces between droplets.

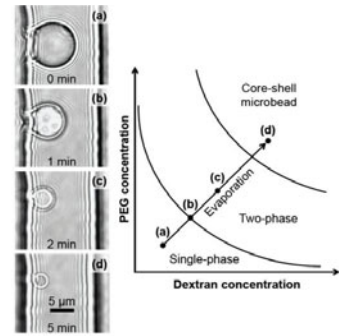

Figure 1 (a) A single-phase droplet of 1% PEG and 1% dextran experienced a series of evaporation-induced phase transitions to: (b) initial phase nucleation, (c) complete aqueous two-phase separation, and (d) core–shell microbead. Adapted from Ref. 12 with permission from The Royal Society of Chemistry.

Aqueous two-phase microdroplets with reversible phase transitions

Two-phase systems contained within microdroplets are being adapted by many groups as models for dynamic microcompartmentation and affinity partitioning of biomolecules. Creation of aqueous two-phase systems was enabled by coalescing two or more femtoliter-volume droplets produced on-demand in a microchannel, each having a different high molecular weight polymer which is miscible in water. [12]

In contrast to other reports of aqueous two-phase microdroplets, which rely on continuous flows/jets and high-frequency droplet formation, [13] our device exploits the interfacial tension between the oil and aqueous phases to generate ultrasmall two-phase droplets with a well-defined time zero and without crossflow in the oil phase. This allows us to monitor individual droplets for extended times, and to carry out programmed sequential phase transitions on the same droplet.

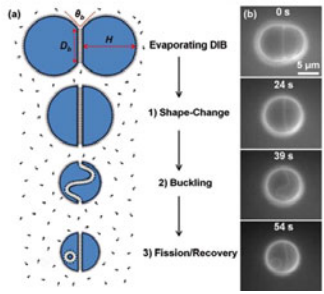

Figure 2 (a) Schematic and (b) fluorescent imaging of an evaporating µDIB experiencing buckling and fission. During droplet evaporation, lipids transfer from the monolayers to the bilayer, resulting in bilayer confinement, buckling, and fission. Adapted with permission from Ref. 14. Copyright 2013 American Chemical Society.

As shown in Figure 1, single-phase droplets containing initially low polymer concentrations (1% PEG and 1% dextran), transition to two-phase droplets as the polymer concentrations in the droplets increase past the single-phase / two-phase coexistence line. This was due to shrinking of the droplets caused by rapid loss of water from the droplet from evaporation. As the droplet continues to shrink, there is another transition to core–shell microbeads once the entire amount of water in the droplet has disappeared. These phase transitions are fully reversible upon rehydration by fusion with additional droplets of water.

Buckling and fission of microscale lipid bilayers in femtoliter-volume droplets

As an extension of the work on ATPS microdroplets, we created microscale droplet interface bilayers (μDIBs), formed as described above for APTS droplets, by injecting aqueous droplets from apposing nanochannels into an oil-filled main channel, as shown with Figure 2. [14] Droplet interface bilayers (DIBs) consist of two or more aqueous droplets in oil, each covered with a monolayer of lipids. When two or more of these droplets encounter each other, a lipid bilayer can spontaneously form at the point of contact. DIBs are convenient systems for electrical characterizations of membranes, and for the option to create asymmetric bilayers by connecting two or more droplets with different compositions. DIBs are usually assembled manually, by connecting millimeter-scale droplets using pipettes, electrodes or lasers.

Depending on whether the lipid molecules were initially present in the water droplets as liposomes ("lipid-in"), or in the oil phase as reverse micelles and emulsified aggregates ("lipid-out"), we identified three distinct classes of lipid transfer that occurred with μDIBs during evaporation that were dependent on the initial conditions of the system. The first class consisted of buckling and fission of the bilayer. As both droplets lost volume due to evaporation in the channel, monolayer interfaces changed shape to assume the most energetically favorable configuration: a single spherical droplet partitioned into two hemispheres by the lipid bilayer. Bilayer growth was fueled by the shrinkage of the monolayer interfaces, which forced lipids in the monolayers to pair together and slide into the bilayer like a conveyor belt. Increased confinement due to evaporation of water resulted in buckling of the bilayer. Ultimately, fission of membrane material to produce a daughter vesicle at the critical radius of curvature and bending moment required for pinch-off occurred.

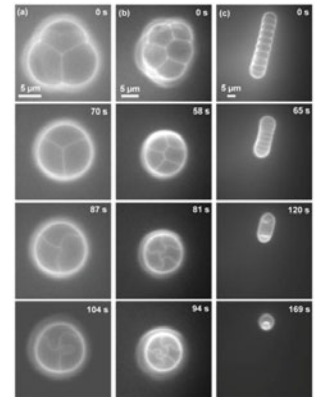

Figure 3. μDIBs networks: (a) 3-droplet cluster, (b) 5-droplet cluster, (c) 10-droplet chain. Adapted from Ref. 15 with permission from The Royal Society of Chemistry.

Figure 3 displays some of the clusters that could be formed from multiple μDIBs, including a 3-droplet cluster configuration, a 5-droplet cluster, or a 10-droplet chain. [15] For the 3-droplet cluster, the system still evaporated into the shape of a single sphere, but now the interior was partitioned into three equivalent compartments by three bilayers. Similarly, the 5-droplet cluster evaporated into a sphere with five compartments. Chain configurations occurred when more droplets were con-nected together, such as the 10 droplet case shown in Figure 3. In this case, the chain could not morph into a single spherical shape because of the intermediate bilayers, which would have to be ruptured in order to bring all the droplets together. Therefore, the droplets preferred to longitudinally shrink from both ends toward the center of the chain. For the 3-droplet and 5-droplet clusters, all bilayers buckled in tandem as they became confined inside of the sphere. In contrast, the bilayers in the chain network preferentially grew and buckled at the ends of the chain. This was due to the interfacial area of the monolayers being greater at the ends of the chain, resulting in enhanced evaporation and shape-change compared to the middle of the chain. As evaporation continued, lipid bilayers in the middle of the chain also became confined, inducing buckling in a chain reaction that propagated from the ends of the chain towards the middle.

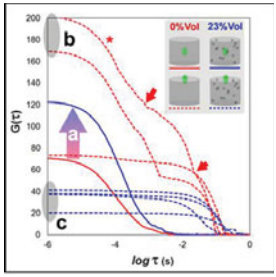

Figure 4. Four families of fluorescence correlation curves show how combined effects of crowding and molecule-wall interactions result in longer correlation times than either effect alone. Reproduced from Ref. 16 with permission from The Royal Society of Chemistry.

For droplet clusters and chains, fission could not be observed due to the buckling bilayers contacting adjacent monolayers and/or bilayers before reaching the critical radius of curvature. As the buckling bilayer contacts another interface, budding can occur, which creates new interfacial area that can better manage stress.

Single-molecule mobility in confined and crowded femtoliter chambers

We studied the effects of systematically increasing crowding and confinement on the mobility of small fluorescent molecules in aqueous solution with Fluorescence Correlation Spectroscopy (FCS), and compared these to three-dimensional stochastic Monte Carlo simulations. [16] For this experiment, we employed chambers micromolded in PDMS that could be closed in milliseconds with a pressure pulse acting on the channel containing the chambers, trapping solution containing the fluorophore in several, identical wells. We found that when crowding (using the inert macromolecule Ficoll-70) and the degree of confinement were increased simultaneously, extended correlation times of fluorescent intensity fluctuations measured with FCS were observed. This was not the case when confinement or crowding was observed separately. Both experiment and simulation indicate that even without crowding, diffusional mobility decreases with increasing confinement due to increased molecule-wall interactions. However, as depicted in Figure 4, these interactions became amplified in the presence of the crowders, which significantly extended the average time fluorophores were trapped at the wall.

Sealable, femtoliter chamber arrays for cell-free biology

Cell-free expression systems provide a flexible platform for probing specific networks of biological reactions isolated from the complexity of resource sharing in cells. However, at the macroscale, these systems do not exhibit the same levels of effectiveness as biological systems at the microscale. To better understand the roles that internal structure and scale have on reaction dynamics, we measured the same noise structure of a cell-free system as that carried out on cellular systems. [17] We confined *E. coli* cell-free extract in the same cell-sized microfluidic chambers in PDMS as described in the previous section, as well as in lipid vesicles, to explore how confinement affects protein expression. At cellular scales, gene expression is bursty, which involves periods in time of high expression separated by intervals where expression is negligible. Time-variant

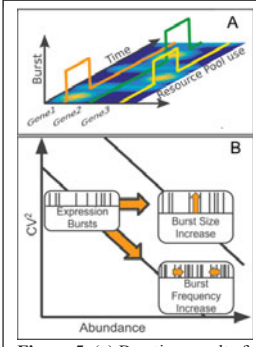

Figure 5. (a) Bursting results from having limited pool of expression resources in confined environments. (b) Resources may be shared by all genes in a single, large volume, or by compartmentalization in smaller, summed volumes. Adapted with permission from Ref. 17. Copyright 2016 American Chemical Society.

expression bursting in cells is a consequence of having a limited reservoir of expression resources (ribosomes, polymerases, nucleic acids, etc.) confined in finite cellular volumes, represented schematically with figure 5(a).

We found that when expression from smaller chambers were summed to match the size of a single larger chamber, the summed smaller chambers increased protein abundance by increasing burst frequency (discrete resource case), while an individual larger chamber increased protein numbers primarily through increases in burst size (shared resource case). The coefficient of variation squared (CV^2), which is the ratio of the variance of protein abundance to the square of the mean, was highly sensitive to the burst frequency but not the burst size, which distinguished the two mechanisms. Protein abundance values where changes in CV^2 varied inversely with protein abundance were indicative of changes in burst frequency, with little or no change in burst size (Figure 5b). On the other hand, changes in protein abundance that induced little or no changes in CV^2 were indicative of changes in burst size, with little or no change in burst frequency. The implication was that for higher protein abundances, it became easier to extend a burst than to initiate a new one, which suggests a role for positive feedback or cooperativity. Similar behavior has been reported in transcription and translation studies in *E. coli*, [18, 19] which suggests bursting is important for optimizing the use of limited, shared resources.

CONCLUSIONS

The integration of micro/nanotechnology with biology is improving our understanding of the design rules governing cell-like complexity and the emergence of functionality at the nanoscale. Included here are recent examples from our group that have highlighted the integration of controllable micro and nanofabricated interfaces with biological systems. Improved understanding of how the chemical activity of water varies under conditions of cellular-scale confinement and crowding will become increasingly important for enabling the next generation of synthetic biological hybrid systems having precise spatiotemporal control of molecular transport, binding interactions, assembly, and catalysis, with single-molecule resolution and sensitivity.

ACKNOWLEDGMENTS

This research was conducted at the Center for Nanophase Materials Sciences, which is a DOE Office of Science User Facility.

REFERENCES

1. R.J. Ellis, Trends Biochem. Sci. 26, 597 (2001).
2. S.B. Zimmerman, and A.P. Minton, Annu. Rev. Biophys. Biomol. Struct. 22, 27 (1993).
3. D. Hall, and A.P. Minton, Biochim. Biophys. Acta 1649, 127 (2003).
4. H.-X. Zhou, G. Rivas and A.P. Minton, Annu. Rev. Biophys. 37, 375 (2008).
5. S. Cayley, and M.T. Record Jr., J. Mol. Recognit. 17, 488 (2004).
6. J.A. Dix, and A.S. Verkman, Annu. Rev. Biophys. 37, 247 (2008).
7. J.T. Mika, B. Poolman, Curr. Opin. Biotechnol. 22, 117 (2011).
8. O. Bénichou, C. Chevalier, J. Klafter, B. Meyer, and R. Voituriez, Nat. Chem. 2, 472 (2010).

9. Z.A. Schuss, D. Singer, and D. Holcman, Proc. Natl. Acad. Sci. USA 104, 16098 (2007).
10. A. Singh, and L.S. Weinberger, Curr. Opin. Microbiol. 12, 460 (2008).
11. V.A. Parsegian, R.P. Rand and D.C. Rau, Proc. Natl. Acad. Sci. USA 97, 3987 (2000).
12. J.B. Boreyko, P. Mruetusatorn, S.T. Retterer, and C.P. Collier, Lab Chip 13, 1295 (2013).
13. S. Ma, J. Thiele, X. Liu, Y. Bai, C. Abell and W. T. S. Huck, Small, 8, 2356 (2012).
14. J.B. Boreyko, P. Mruetusatorn, S.A. Sarles, S.T. Retterer, and C.P. Collier, J. Am. Chem. Soc. 135, 5545 (2013).
15. P. Mruetusatorn, J.B. Boreyko, G. Venkatesan, S.A. Sarles, D. Hayes, and C.P. Collier, Soft Matter 10, 2530 (2014).
16. J.D. Fowlkes and C.P. Collier, Lab Chip 13, 877 (2013).
17. P.M. Caveney, S.E. Norred, C.W. Chin, J.B. Boreyko, B.S. Razooky, S.T. Retterer, C.P. Collier, and M.L. Simpson, ACS Synth. Biol. 6, 334 (2016).
18. L. So, A. Ghosh, C. Zong, L.A. Sepúlveda, R. Sergev, and I. Golding, Nat. Genet. 43, 554 (2011).
19. R.D. Dar, B.S. Razooky, L.S. Weinberger, C.D. Cox, and M.L. Simpson, PLoS One 10, e0140969 (2015).